NANO LETTERS

Letter

pubs.acs.org/NanoLett

van der Waals Epitaxy of InAs Nanowires Vertically Aligned on Single-Layer Graphene

Young Joon Hong,*[,†] Wi Hyoung Lee,[‡] Yaping Wu,[‡] Rodney S. Ruoff,*[,‡] and Takashi Fukui*[,†]

[†]Research Center for Integrated Quantum Electronics (RCIQE) and Graduate School of Information Science and Technology, Hokkaido University, Sapporo 060-8628, Japan

[‡]Department of Mechanical Engineering and the Materials Science and Engineering Program, The University of Texas at Austin, Austin, Texas 78712, United States

Supporting Information

ABSTRACT: Semiconductor nanowire arrays integrated vertically on graphene films offer significant advantages for many sophisticated device applications. We report on van der Waals (VDW) epitaxy of InAs nanowires vertically aligned on graphene substrates using metal−organic chemical vapor deposition. The strong correlation between the growth direction of InAs nanowires and surface roughness of graphene substrates was investigated using various graphene films with different numbers of stacked layers. Notably, vertically well-aligned InAs nanowire arrays were obtained easily on single-layer graphene substrates with sufficiently strong VDW attraction. This study presents a considerable advance toward the VDW heteroepitaxy of inorganic nanostructures on chemical vapor-deposited large-area graphenes. More importantly, this work demonstrates the thinnest epitaxial substrate material that yields vertical nanowire arrays by the VDW epitaxy method.

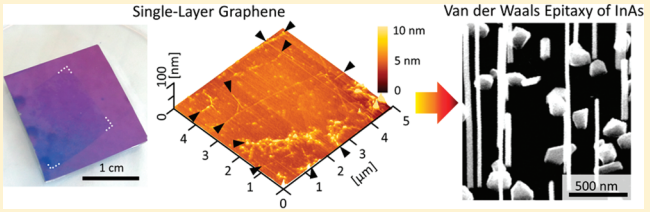

KEYWORDS: *van der Waals epitaxy, graphene, InAs, vertical nanowire, heterostructures, metal−organic vapor-phase epitaxy*

Hybrid junctions composed of semiconductor nanostructures and graphene have received much attention because of their excellent material properties and unique junction characteristics, which can be exploited for many functional device applications.[1−4] Heteroepitaxy of semiconductor nanomaterials on graphene (or vice versa) is a direct and scalable route for integration into more sophisticated devices.[5−8] However, the rationale for direction- and size-controlled heteroepitaxy of semiconductor nanostructures on graphene has rarely been studied, although precisely controlled objects are required in many integrated device fabrications. Graphene is a promising substrate material for flexible and transparent device applications due to excellent optical transparency and electrical conductivity,[9−12] and chemical vapor deposition (CVD) has opened a new route for large-scale production of high-quality graphene films in practical applications.[13] Furthermore, the large-scale production of CVD-grown graphene on arbitrary substrates has increased the versatility of graphene as a substrate.[14,15] The advantages of CVD-grown large-area graphene make it well suited for the high productivity of metal−organic vapor-phase epitaxy (MOVPE). Hence, a combined CVD and MOVPE process can be used to advance the monolithic integration of semiconductor nanostructures on graphene. In this Letter, we demonstrate vertically well-aligned InAs nanowire arrays grown by van der Waals (VDW)−MOVPE on large-area single-layer graphene (SLG) films. Additionally, we report the effect of the surface roughness of graphene on the control of nanowire growth direction.

Recently, we reported the quasi-VDW heteroepitaxy as a method for growing the nonoxide nanostructures on nonwetting graphite surface, and we have also demonstrated critical factors leading to the preferential nucleation and epitaxial growth of either nanowire or island morphology, namely (1) the surface potential wells formed by surface ledges and (2) the nearly coherent heteroepitaxial relationship.[16] Accordingly, it has been proven that the graphite layers, composed of many $\pi-\pi$ stacked graphene layers, can provide the substantial VDW attraction for epitaxy of InAs nanostructures thereon. However, since the surface potential significantly decreases with decreasing the graphene thickness, measured by electrostatic force microscopy,[17] it may be rewarding to investigate how ultrathin graphene layers can be used as substrates for the VDW heteroepitaxy. Herein, we present the one-atom-thick graphene substrates, which are the thinnest substrate material, yielding vertical nanowire arrays by the VDW epitaxy method.

InAs nanowires were grown on graphene films by the VDW heteroepitaxy[18] using catalyst-free MOVPE. For substrate preparation, 1.5 cm ×1.5 cm SLG[19] and multilayer graphene (MLG) films[20,21] were synthesized on 25 μm thick copper (Cu, Alfa Aesar, item No. 13382) and 200 μm thick copper−nickel alloy (Cu−Ni, composed of Ni 31.00 wt %, Cu 67.80 wt %, Fe 0.60 wt %, Mn 0.45 wt %, and Zn 0.07 wt %, All Metal Sales, Inc.) or nickel foils, respectively, by CVD, and transferred onto

Received: November 22, 2011
Revised: January 26, 2012
Published: February 10, 2012

   dx.doi.org/10.1021/nl204109t | *Nano Lett.* 2012, 12, 1431−1436

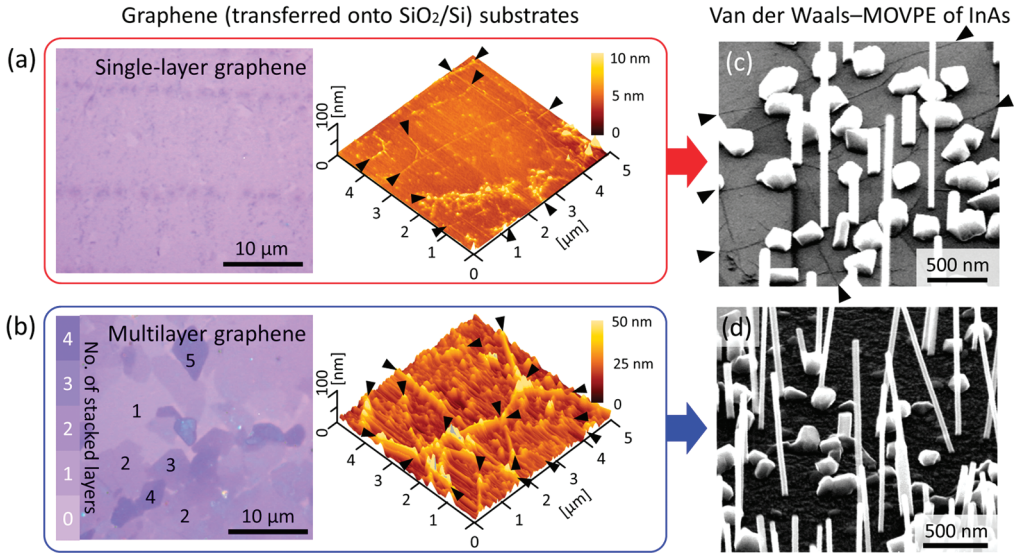

Figure 1. InAs nanowires grown on CVD-grown graphene substrates. Optical microscopic image and AFM surface topographic map of (a) SLG and (b) MLG films. Tilt-view FE-SEM images of InAs nanowires grown on (c) SLG and (d) MLG substrates. The wedges indicate graphene wrinkles.

SiO_2/Si substrates by metal etching and transfer techniques[14] for high-temperature MOVPE. The SLG and MLG films were grown in hot wall and cold wall reactor furnaces, respectively, at growth temperature of 975−1030 °C using a mixture of methane (CH_4) and hydrogen (H_2). We note that the growth temperature as well as cooling rate is very important in controlling the thickness and roughness of graphene layers.[20] Graphene-deposited metal foil samples were spin-coated with poly(methyl methacrylate) (PMMA), and graphene films were taken away from the metal foils by etching in an aqueous solution of iron nitrate [$Fe(NO_3)_3$ (1 M)]. Overnight etching yielded a film floating on the solution surface due to high surface tension. The 285 nm thick SiO_2-coated Si substrates were used to capture and support the floating films that were then dried in air. After the transfer process, graphene on SiO_2/Si substrate was obtained by removing the PMMA using acetone. In order to further remove the residues of PMMA, the substrates were annealed at 400 °C for 1 h in mixture of H_2 and argon.[22] Prior to InAs growth, thermal cleaning was carried out at 600−650 °C for 10 min under ambient H_2 to remove adsorbates or contaminants formed on the graphene surface in air. Immediately after thermal cleaning, the MOVPE reactor was purged by AsH_3 with a typical flow rate of 100 sccm (denotes standard cubic centimeter per minute) at 410 °C, and repetitive flow-rate-modulated cycles were performed during temperature ramping from 410 to 560 °C.[23] Subsequently, the InAs nanowires were grown at 560 °C for 20 min. The total flow rate of the gases was maintained at 5.75 slm (standard liter per minute) during the MOVPE process. For the growth of InAs nanowires, trimethyl−indium and 5%-AsH_3 diluted with H_2 were used as precursors with the typical flow rates of 10 and 100 sccm, respectively. The thickness and uniformity of graphene films on SiO_2/Si substrates were evaluated using Raman spectroscopy (λ = 532 nm) and optical microscopy to confirm the number of stacked layers in the graphene films. Surface morphological analyses of the graphene substrates and InAs nanowires were performed using atomic force microscopy (AFM, Veeco Nanoscope Multimode SPM) and field-emission scanning electron microscopy (FE-SEM, Hitachi S-4100), respectively. The AFM surface topographic maps of graphene films were obtained after the removal of PMMA residues by annealing the substrates in H_2/Ar mixture. Microstructural analyses were carried out using high-resolution transmission electron microscopy (HR-TEM, Hitachi H-9000UHR). For cross-sectional TEM imaging and electron diffraction analyses, samples were milled using both argon ion milling machine (Gatan 600N Duomill) and focused ion beam machine (FIB, Hitachi FB-2100 m and FEI STRATA DB235). The incident electron beam was directed along the InAs $\langle 1\bar{1}0 \rangle$ orientation to define the crystal structure of InAs nanowires in the TEM inspections.

Figure 1 shows photographs and surface topographic maps of CVD-grown SLG (Figure 1a) and MLG (Figure 1b) films transferred onto SiO_2/Si substrates for VDW−MOVPE growth of InAs nanowires. The photomicrograph in Figure 1a shows that the transferred SLG films exhibited extremely uniform color and contrast over the entire surface, indicating the uniform thickness and high quality of the SLG films, whereas the MLG films had many dappled areas with uneven contrast due to inhomogeneous thickness (left panel of Figure 1b). Raman spectra as well as cross-sectional TEM image confirm the thickness and crystal quality of SLG films (Figure S1 and S2, Supporting Information). The surface topographies measured by AFM clearly show different surface roughness values and wrinkle heights for the SLG and MLG films (right panels in Figure 1a,b). Since the difference of thermal expansion coefficients between metal foil and deposited graphene layer causes the graphene wrinkles to release thermal stress during quenching, higher growth temperature of the MLG films has resulted in denser and taller wrinkles than those of SLG films.[20,24] The root-mean-square (rms) roughness values of SLG, $MLG_{(Cu-Ni)}$, and MLG_{Ni} films were measured to be 2.4 ± 0.6, 12.0 ± 8.8, and 20.5 ± 13.8 nm, respectively (the subscripts of Cu−Ni and Ni denote the catalyst foils used for the synthesis of graphene, and ± represents the standard deviation), while the wrinkle heights of the SLG and MLG films ranged from 2 to 8 and 5 to 60 nm, respectively (Table 1). For the wrinkle-free areas of the graphene films, the rms surface roughness values of SLG, $MLG_{(Cu-Ni)}$, and MLG_{Ni} were measured to be 0.5 ± 0.2, 2.9 ± 0.7, and 6.8 ± 2.2 nm (Table

dx.doi.org/10.1021/nl204109t | Nano Lett. 2012, 12, 1431−1436

Table 1. Summary of Surface Morphological Characteristics of CVD-Grown Graphene Films Used for Growth of Vertical InAs Nanowire Arrays

substrate	rms surface roughness[a] [nm]	rms surface roughness of wrinkle-free area [nm]	Wrinkle height [nm]
SLG	2.4 ± 0.6	0.5 ± 0.2	2–8
$MLG_{(Cu-Ni)}$	12.0 ± 8.8	2.9 ± 0.7	5–40
MLG_{Ni}	20.5 ± 13.8	6.8 ± 2.2	5–60

[a]The values were determined by AFM, measured on a crack-free area of 20 μm × 20 μm.

1), respectively, indicating that thicker films exhibited higher surface roughness due to the presence of many graphene ledges, as seen in the photomicrograph of MLG in Figure 1b. The number of stacked layers in the graphene films increased locally during CVD, increasing the surface roughness and ledges (or kinks) of MLG.

The FE-SEM images of Figure 1c,d show the general morphologies of InAs nanowires grown on SLG and MLG substrates, respectively (also Figure S3, Supporting Information). The VDW heteroepitaxy of InAs yielded vertically well-aligned nanowire arrays on SLG films with a typical nanowire number density of (1.6 ± 0.7) × 10^8 cm^{-2}, whereas the same VDW growth conditions resulted in vertically less-aligned nanowires on MLG films with an increased number density of (6.9 ± 1.1) × 10^8 cm^{-2}. On the SiO_2 surfaces, randomly oriented nanowires formed with a nanowire number density of ca. 10^7 cm^{-2} (Figure S5, Supporting Information). Much higher number density of nanowires grown on SLG than those on SiO_2 surface presumably indicates that the electrostatic attractions from the underneath SiO_2 layer is almost negligible for the VDW heteroepitaxy. According to the intermolecular attractions, since the potential decreases with interdistance as r^{-n} ($n \sim 2-6$, depending on type of dipole) far more rapidly than the ionic bonding potential, which decreases only as r^{-1}, the heterointerfacial attractions in the VDW heteroepitaxy is attributable mostly to the topmost SLG films. The excellent vertical alignment of the nanowires on graphene suggests an epitaxial relationship between InAs and graphene. The as-grown vertical nanowires on graphene substrates did not exhibit tapering (Figure 1c,d), and the typical nanowire diameter was measured to be 40 ± 14 nm (Figure S4, Supporting Information), indicating well-optimized VDW–MOVPE conditions for InAs nanowire growth. Note that the CVD-grown graphene wrinkles did not cause preferential nucleation and growth of unwanted InAs island structures, which are distinct from the high-density growth of InAs islands along the step-edges of cleaved graphite flakes.[16] This implies that the unwanted formation of island crystals can be suppressed using CVD-grown graphene substrates.

Figure 2a shows the top-view FE-SEM image of InAs nanowires grown on SLG films, revealing that the neighboring nanowires, all of which exhibited a hexagonal prismatic morphology with six zinc blende-{$\bar{1}$01} sidewall facets, had an identical 6-fold rotational in-plane alignment within a single domain of the SLG due to the heteroepitaxial relationship between InAs and SLG. As schematically presented in Figure

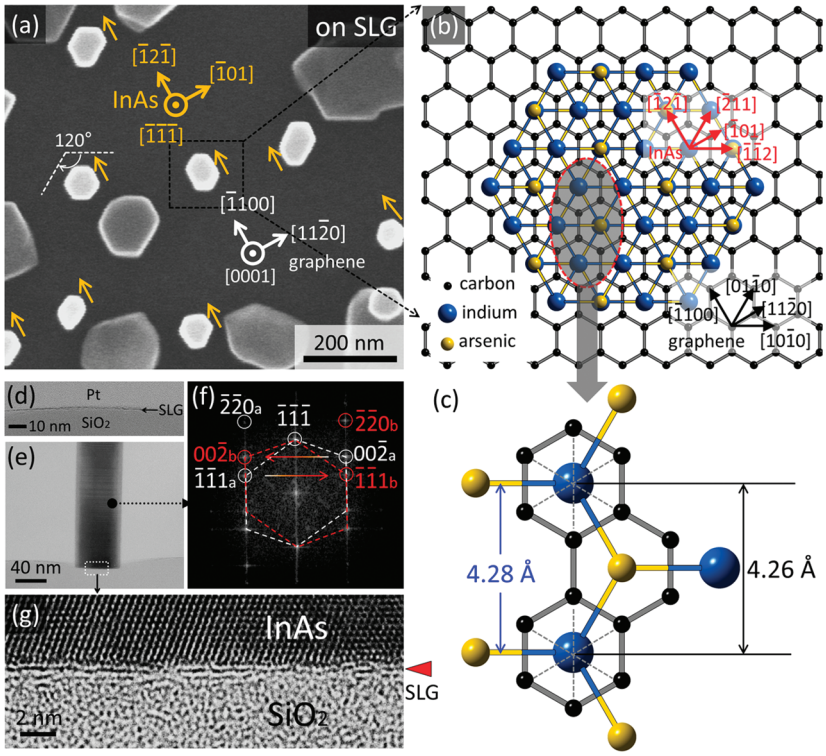

Figure 2. Vertically well-aligned InAs nanowires heteroepitaxially grown on SLG. (a) Top-view FE-SEM image of InAs nanowires grown heteroepitaxially on SLG films. Brighter structures are nanowires with a hexagonal prismatic shape. (b,c) Schematic images of the atomic configuration presenting the nearly coherent heteroepitaxial relationship of zinc blende InAs-($\bar{1}$11)[$\bar{1}$10]||SLG-(0001)[1$\bar{2}$10]. (d) Cross-sectional TEM image of SLG film transferred onto a SiO_2/Si substrate. (e) Low-magnification cross-sectional TEM image of InAs nanowire vertically grown on SLG. (f) Selected-area diffraction pattern obtained through a FFT process of the HR-TEM image of nanowire. (g) HR-TEM image of the enclosed area in (e), showing the interface of InAs/SLG/SiO_2.

dx.doi.org/10.1021/nl204109t | Nano Lett. 2012, 12, 1431–1436

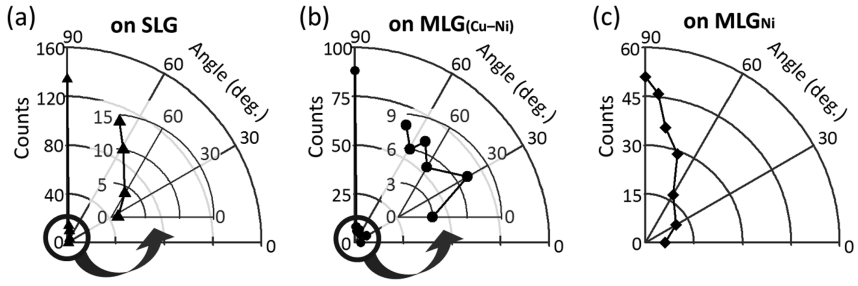

Figure 3. Polar histograms presenting the spatial distribution of the growth direction of InAs nanowires grown on (a) SLG, (b) $MLG_{(Cu-Ni)}$, and (c) MLG_{Ni}.

2b,c, the distance of the nearest InAs primitive lattices (In−As dimers) along the zinc blende $\langle \bar{1}10 \rangle$ is 4.28 Å, which is almost equivalent to the distance of the nearest-neighbor carbon honeycomb lattices along the $\langle 1\bar{2}10 \rangle$ in the graphene layer (≈4.26 Å).[25] Those values have only a small misfit of ∼0.5%. Therefore, we believe that the nearly coherent heteroepitaxial relationship of InAs-$(\bar{1}\bar{1}\bar{1})[\bar{1}10]$||graphene-$(0001)[1\bar{2}10]$ allowed the ultrathin SLG films to provide sufficiently strong VDW attraction, forming the vertical nanowires.

In order to explore the microstructure and heterointerface of InAs nanowires and SLG, cross-sectional TEM analyses were carried out. First, we inspected the SLG films transferred onto SiO_2/Si substrates using TEM. Figure 2d exhibits that the SLG film consists mostly of monoatomic layer (bilayers were partly observed in SLG films, Figure S2, Supporting Information). Figure 2e displays the cross-sectional TEM image of a typical InAs nanowire vertically formed on SLG film, showing a uniform diameter of nanowire (∼55 nm). Selected area diffraction pattern, which was obtained by a fast Fourier transform (FFT) process of the HR-TEM image of InAs nanowire, exhibits that the nanowire grew along the zinc blende $[\bar{1}\bar{1}\bar{1}]$ orientation, perpendicular to the SLG(0001) surface (Figure 2f) with many twin planes. However, it is notable that InAs nanowires formed straight with a fairly uniform diameter along the entire length of nanowire in spite of the formation of twin planes. This signifies that the initially formed bottom layer determines the plan-view shape of nanowire. As seen in Figure 2a, the nanowires exhibit slightly irregular hexagonal prismatic shapes in the plan view. This irregular shape formation of nanowires is not resulted from polytypism nor twin planes, but can be ascribed to locally inhomogeneous hydrophobic surface of the graphene substrate, promoting the heteroepitaxial formation of irregular hexagon initial layers. Figure 2g is the HR-TEM image taken at the heterointerface of bottom of InAs nanowire/SLG/SiO_2 layer, clearly showing the abrupt heterointerfaces of InAs and graphene. The image also displays that the SLG substrate consists of 1−2 atomic layers. The bilayers observed in the SLG are presumably attributed to inhomogeneous thickness of the SLG and/or difficulty in taking a perfect tomographic TEM picture with such a thick sample (∼60 nm) sliced by the FIB. Importantly, no threading dislocations were found at the VDW heterointerfaces, owing to either the weakly bound VDW attractions or the nearly coherent heteroepitaxial relationship between InAs (111) and graphene surfaces.

The growth direction of InAs nanowires was examined using graphene films with different numbers of stacked layers. The polar histograms in Figure 3 show the distributions of the growth direction angle of InAs nanowires grown on SLG, $MLG_{(Cu-Ni)}$, and MLG_{Ni} surfaces. Among the substrates, SLG resulted in excellent vertical alignment of the InAs nanowires (Figures 3a and 1c), presumably due to the flat, smooth surface of SLG films. In contrast, the MLG films yielded vertically less-aligned nanowire arrays (Figure 3b,c). We further compared the vertical alignment of InAs nanowires grown on the SiO_2 surface as a control experiment (Figure S5b, Supporting Information), and the SiO_2 surface resulted in randomly oriented nanowire arrays due to the lack of an epitaxial relationship between InAs and amorphous SiO_2. Figure 3 clearly exhibits that the nanowire vertical alignment was deteriorated as employing thicker graphene substrates (also Figure S3, Supporting Information). This trend may not be resulted simply from the graphene thickness but from the roughness of graphene films.

The vertical alignment of nanowire arrays depended strongly on the number of stacked layers in the graphene films. As shown in the photomicrographs and AFM topographies in Figure 1a,b and Table 1, the thicker graphene films exhibited higher surface roughness with many graphene ledges (or kinks) because the MLG films mostly consisted of partly thickly formed graphene layers (Figure 1b) that result in inhomogeneously thick graphene layers with many ledges or kinks. Accordingly, we assumed that the ledges (or kinks) in wrinkle-free area, as a source of graphene roughness, determine the nucleation density and growth direction of InAs nanowires. Note that the graphene wrinkles did not promote the growth of InAs. The correlation between the vertical alignment of InAs nanowires and the surface roughness of graphene surfaces was explored. In this investigation, only the nanowires grown with standing angles of 90 ± 5° from the substrate surface were presumed to be vertically aligned. Figure 4 shows that extremely flat graphene surfaces resulted in vertically well-aligned nanowire arrays with a nearly 100% vertical yield,[26] and the vertical alignment deteriorated as a function of the rms roughness of the graphene substrates (black solid circles in Figure 4). The number density of the nanowires increased as graphene roughness increased (blue empty squares in Figure 4). The two correlations demonstrate that rough graphene surfaces, caused by graphene ledges, facilitate the heterogeneous nucleation and growth of InAs nanowires on nonwetting graphene surfaces but highly rough ledges deteriorate the vertical growth of nanowires due to weakly bound VDW heterojunctions between InAs and graphene. The VDW nucleation−growth of nanowires on graphene ledges (or kinks) is consistent with our previous report on nanowire growth on bulk graphite.[16] We therefore surmise that not only the graphene ledges but also the vacancies or point defects in SLG can be the heterogeneous nucleation sites for the VDW epitaxy of nanowires because such interplanar defects promote the consecutive process of (i) adatom−vacancy (or adatom−ledge, adatom−kink) pair formation,[27,28] (ii) heterogeneous

dx.doi.org/10.1021/nl204109t | Nano Lett. 2012, 12, 1431−1436

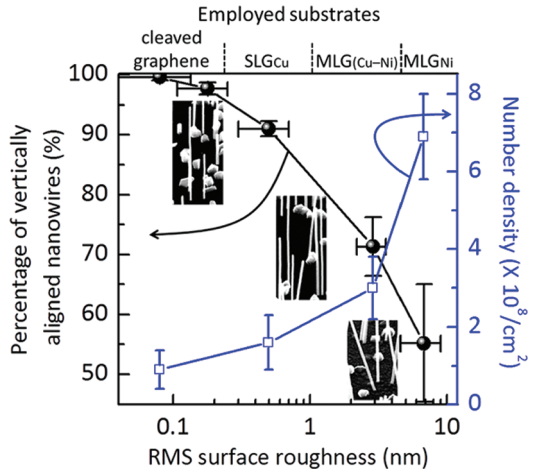

Figure 4. Plot of the percentage yield of vertically well-aligned InAs nanowires (black solid circles) and number density of the nanowires (blue empty squares) as a function of the rms surface roughness of the graphene substrates. The roughness values were measured on wrinkle-free areas of the graphene substrates.

nucleation, and (iii) heteroepitaxial growth of nanowires.[16] The surface flatness of graphene substrates with controlled surface potential is of great importance for the VDW epitaxy of vertically well-aligned InAs nanowire arrays.

Vertical growth of InAs nanowires was achieved on large-area flat graphene with the nearly lattice-matched epitaxial relationship between InAs and graphene. Graphene has advantageous characteristics as a substrate for nanowire epitaxy. First, nanowire morphologies and a narrow diameter distribution (~40 ± 14 nm, Figure S4, Supporting Information) can be easily obtained without the use of mask patterns, presumably due to the limited coalescence size of InAs on the hydrophobic graphene surface. Second, owing to noncovalent bonding at the heterojunction of InAs and graphene, the VDW epitaxy preferentially produces vertical InAs nanowires exclusively along zinc blende [111]B on flat graphene and even on damaged, rough graphene surfaces. This is quite distinct from Si substrates, which can have either arsenic- or indium-terminated Si^{1+} or Si^{3+} structures, and the termination determines the InAs nanowire growth direction from among a few specific directions.[23] Hence, graphene substrates can be exploited for fabricating polar/nonpolar semiconductor heterostructures[29] with easily controlled nanowire growth direction using the VDW epitaxy method, regardless of the surface termination of substrate.

Vertical growth of InAs nanowires on large-area SLG films was demonstrated using VDW epitaxy. High-quality graphene is critical for obtaining vertically well-aligned InAs nanowires. The use of SLG with a smooth surface allowed us to grow vertically well-aligned InAs nanowires with a vertical yield greater than 90%, demonstrating the feasibility of SLG films as epitaxial substrates. The combination of VDW–MOVPE and CVD-grown large-area graphene can be used to facilitate heteroepitaxy of vertical inorganic nanostructure arrays on graphene films for many functional device applications. More generally, the thinnest material, that is, the one-atom-thick graphene, shall be readily exploited as epitaxial substrates for developing many unconventional sophisticated devices in a flexible, transparent form.

■ ASSOCIATED CONTENT

Ⓢ Supporting Information

Supporting figures and descriptions for Raman spectra of SLG and MLG films used as substrates (S1); cross-sectional HR-TEM image of SLG film used for substrates (S2); low-magnification SEM images of InAs nanowires grown on various graphene substrates (S3); diameter histogram of InAs nanowires grown on SLG films (S4); typical surface morphologies and growth directions of InAs nanowires grown on SiO_2 layers (S5). This material is available free of charge via the Internet at http://pubs.acs.org.

■ AUTHOR INFORMATION

Corresponding Author

*E-mail: (Y.J.H) yjhong@rciqe.hokudai.ac.jp; (R.S.R) r.ruoff@mail.utexas.edu; (T.F.) fukui@rciqe.hokudai.ac.jp.

Notes

The authors declare no competing financial interest.

■ ACKNOWLEDGMENTS

This work was financially supported by the Japan Society for the Promotion of Science (JSPS) through the JSPS postdoctoral fellowship for foreign researchers (ID No. P11363). The authors thank Professors J. Motohisa and S. Hara for their valuable comments and discussions. We also acknowledge Dr. K. Tomioka for his support of MOVPE experiments.

■ REFERENCES

(1) Kim, K.; Choi, J.-Y.; Kim, T.; Cho, S.-H.; Chung, H.-J. *Nature* **2011**, *479*, 338–344.
(2) Ci, L.; Song, L.; Jin, C.; Jariwala, D.; Wu, D.; Li, Y.; Srivastava, A.; Wang, Z. F.; Storr, K.; Balicas, L.; Liu, F.; Ajayan, P. M. *Nat. Mater.* **2010**, *9*, 430–435.
(3) Lee, J. M.; Choung, J. W.; Yi, J.; Lee, D.; Samal, M.; Yi, D. K.; Lee, C.-H.; Yi, G.-C.; Paik, U.; Rogers, J. A.; Park, W. I. *Nano Lett.* **2010**, *10*, 2783–2788.
(4) Choi, D.; Choi, M.-Y.; Choi, W. M.; Shin, H.-J.; Park, H.-K.; Seo, J.-S.; Park, J.; Yoon, S.-M.; Chae, S. J.; Lee, Y. H.; Kim, S.-W.; Choi, J.-Y.; Lee, S. Y.; Kim, J. M. *Adv. Mater.* **2010**, *22*, 2187–2192.
(5) Kim, Y.-J.; Lee, J. H.; Yi, G.-C. *Appl. Phys. Lett.* **2009**, *95*, 213101.
(6) Dang, W.; Peng, H.; Li, H.; Wang, P.; Liu, Z. *Nano Lett.* **2010**, *10*, 2870–2876.
(7) Chung, K.; Lee, C.-H.; Yi, G.-C. *Science* **2010**, *330*, 655–657.
(8) Park, J.-U.; Nam, S.; Lee, M.-S.; Lieber, C. M. *Nat. Mater.* **2011**, *11*, 120–125.
(9) Novoselov, K. S.; Jiang, Z.; Zhang, Y.; Morozov, S. V.; Stormer, H. L.; Zeitler, U.; Maan, J. C.; Boebinger, G. S.; Kim, P.; Geim, A. K. *Science* **2007**, *315*, 1379.
(10) Park, W. I.; Lee, C.-H.; Lee, J. M.; Kim, N.-J.; Yi, G.-C. *Nanoscale* **2011**, *3*, 3522–3533.
(11) Lee, C.-H.; Kim, Y.-J.; Hong, Y. J.; Jeon, S.-R.; Bae, S.; Hong, B. H.; Yi, G.-C. *Adv. Mater.* **2011**, *23*, 4614–4619.
(12) Kim, R.-H.; Bae, M.-H.; Kim, D. G.; Cheng, H.; Kim, B. H.; Kim, D.-H.; Li, M.; Wu, J.; Du, F.; Kim, H.-S.; Kim, S.; Estrada, D.; Hong, S. W.; Huang, Y.; Pop, E.; Rogers, J. A. *Nano Lett.* **2011**, *11*, 3881–3886.
(13) Bae, S.; Kim, H.; Lee, Y.; Xu, X.; Park, J.-S.; Zheng, Y.; Balakrishnan, J.; Lei, T.; Kim, H. R.; Song, Y. I.; Kim, Y.-J.; Kim, K. S.; Özyilmaz, B.; Ahn, J.-H.; Hong, B. H.; Iijima, S. *Nat. Nanotechnol.* **2010**, *5*, 574–578.
(14) Li, X.; Zhu, Y.; Cai, W.; Borysiak, M.; Han, B.; Chen, D.; Piner, R. D.; Colombo, L.; Ruoff, R. S. *Nano Lett.* **2009**, *9*, 4359–4363.
(15) Lee, Y.; Bae, S.; Jang, H.; Jang, S.; Zhu, S.-E.; Sim, S. H.; Song, Y. I.; Hong, B. H.; Ahn, J.-H. *Nano Lett.* **2010**, *10*, 490–493.

(16) Hong, Y. J.; Fukui, T. *ACS Nano* **2011**, *5*, 7576−7584.
(17) Datta, S. S.; Strachan, D. R.; Mele, E. J.; Johnson, A. T. C. *Nano Lett.* **2009**, *9*, 7−11.
(18) Koma, A. *Thin Solid Films* **1992**, *216*, 72−76.
(19) Li, X.; Cai, W.; An, J.; Kim, S.; Nah, J.; Yang, D.; Piner, R.; Velamakanni, A.; Jung, I.; Tutuc, E.; Banerjee, S. K.; Colombo, L.; Ruoff, R. S. *Science* **2009**, *324*, 1312−1314.
(20) Chen, S.; Cai, W.; Piner, R. D.; Suk, J. W.; Wu, Y.; Ren, Y.; Kang, J.; Ruoff, R. S. *Nano Lett.* **2011**, *11*, 3519−3525.
(21) Cai, W.; Zhu, Y.; Li, X.; Piner, R. D.; Ruoff, R. S. *Appl. Phys. Lett.* **2009**, *95*, 123115.
(22) Lee, W. H.; Park, J.; Sim, S. H.; Lim, S.; Kim, K. S.; Hong, B. H.; Cho, K. *J. Am. Chem. Soc.* **2011**, *133*, 4447−4454.
(23) Tomioka, K.; Motohisa, J.; Hara, S.; Fukui, T. *Nano Lett.* **2008**, *8*, 3475−3480.
(24) Chae, S. J.; Güneş, F.; Kim, K. K.; Kim, E. S.; Han, G. H.; Kim, S. M.; Shin, H.-J.; Yoon, S.-M.; Choi, J.-Y.; Park, M. H.; Yang, C. W.; Pribat, D.; Lee, Y. H. *Adv. Mater.* **2009**, *21*, 2328−2333.
(25) Meyer, J. C.; Geim, A. K.; Katsnelson, M. I.; Novoselov, K. S.; Booth, T. J.; Roth, S. *Nature* **2007**, *446*, 60−63.
(26) Graphene layers with roughnesses of less than 0.3 nm were obtained from step-edge-free graphene flakes mechanically exfoliated from graphite.
(27) Hashimoto, A.; Suenaga, K.; Gloter, A.; Urita, K.; Iijima, S. *Nature* **2004**, *430*, 870−873.
(28) Schäffel, F.; Wilson, M.; Warner, J. H. *ACS Nano* **2011**, *5*, 9428−9441.
(29) Cho, S.; Youn, S. J.; Kim, Y.; DiVenere, A.; Wong, G. K. L.; Freeman, A. J.; Ketterson, J. B. *Phys. Rev. Lett.* **2001**, *87*, 126403.